Interstitial Flow and Its Effects in Soft Tissues

Melody A. Swartz and Mark E. Fleury

Institute of Bioengineering, École Polytechnique Fédérale de Lausanne (EPFL), Switzerland; email: melody.swartz@epfl.ch, mark_fleury@alumni.northwestern.edu

Annu. Rev. Biomed. Eng. 2007. 9:229–56

First published online as a Review in Advance on April 17, 2007

The *Annual Review of Biomedical Engineering* is online at bioeng.annualreviews.org

This article's doi: 10.1146/annurev.bioeng.9.060906.151850

1523-9829/07/0815-0229$20.00

Key Words

transport, mechanobiology, permeability, drug delivery, morphogenesis

Abstract

Interstitial flow plays important roles in the morphogenesis, function, and pathogenesis of tissues. To investigate these roles and exploit them for tissue engineering or to overcome barriers to drug delivery, a comprehensive consideration of the interstitial space and how it controls and affects such processes is critical. Here we attempt to review the many physical and mathematical correlations that describe fluid and mass transport in the tissue interstitium; the factors that control and affect them; and the importance of interstitial transport on cell biology, tissue morphogenesis, and tissue engineering. Finally, we end with some discussion of interstitial transport issues in drug delivery, cell mechanobiology, and cell homing toward draining lymphatics.

Contents

INTRODUCTION

The importance of interstitial flow in physiology has been recognized for more than half a century. One seminal review that has laid the groundwork for this field was that of Levick in 1987 (1), but since that time the understanding of interstitial fluid flow and its effects on solute transport in biological tissues, including effects on cell-cell signaling and morphogenesis, has increased substantially. It is well recognized today that three-dimensional (3-D) in vitro culture better recapitulates in vivo cell physiology than 2-D (2), and in extension we propose that recapitulation of the proper transport environment is also important for persuading in vivo–like cell behavior. Indeed, interstitial flow affects more than just cell nourishment: It can, for example, induce blood and lymphatic capillary morphogenesis in vitro (3–6) and lymphatic regeneration in vivo (7, 8), maintain the functional activity of chondrocytes and osteocytes (9–12), drive fibroblast differentiation (13, 14), and induce cytokine production by smooth muscle cells (15), and interstitial fluid pressure is critical for ocular health (16). Interstitial-like flow helps to promote morphogenesis in perfused organ cultures (17), and small convective flows driven by cilia have been shown to pattern early embryo organ development (18). The aim of this review is to recap some of the most relevant advances and to compile in one location the most important physical laws, material properties, correlations, and measurements dealing with interstitial flow. We

also comment on emerging ideas on how interstitial flow is "sensed" by cells to drive morphogenetic processes and other biological responses.

ECM: extracellular matrix

GAG: glycosaminoglycan

Starling's forces: pressure differences (osmotic and hydraulic) across a vessel wall that drive fluid movement through the vessel wall into the interstitium

THE INTERSTITIAL SPACE

Cells reside in highly specialized extracellular matrices (ECMs) that provide mechanical support, determine mechanical properties, and importantly impart extracellular signals to the cell, both through the ECM molecules and the cytokines that they bind. The specific components of this ECM also vary greatly according to tissue type, but typically include the family of collagens, proteoglycans, laminins, and, in pathological cases, fibrin. The specific composition of the ECM largely determines the resistance to fluid flow, most notably fibrillar collagen and proteoglycans (**Figure 1*a***). Collagen is the most common family of ECM molecules, accounting for more than two-thirds of the ECM protein content of many soft tissues, such as cartilage, dermis, and cornea, and is most abundant in its fibrillar form. Fibrin is a provisional fibrillar matrix found at wound sites and as part of tumor stroma (19). Proteoglycans are large brush-shaped macromolecules that can have molecular masses of several hundred thousand Daltons or more and are constructed of carbohydrates that are often sulfated, known as glycosaminoglycans (GAGs), attached to a protein core (**Figure 1*b***). Common GAGs include heparin, heparan sulfate, chondroitin sulfate, and dermatan sulfate. The highly hydrated and ionic nature of GAGs results in remarkable resistance to compression, an important quality for load-bearing tissues such as cartilage (11), where GAGs are abundant. All of these components can interact both mechanically and covalently and can form 3-D tissue, or as in the case of basal lamina, ordered, layered ECM. In tissue engineering, these are often used in purified form, most commonly fibrin and type I collagen, for 3-D in vitro disease and organ models (20) or in vitro cultured 3-D tissue replacements. Synthetic polymers such as PEG (21) have also found wide use (for reviews see References 22, 23). **Table 1** provides a list of several common ECM components and where they are most abundantly found in the body.

INTERSTITIAL FLUID FLOW

Interstitial Fluid

It is estimated that up to 20% of the body's mass is made up of interstitial fluid (24), and much of this fluid is in constant motion, albeit slowly. In living tissues, interstitial flow is perhaps tied most closely with lymphatic drainage, which returns plasma that has leaked out of the capillaries owing to Starling's forces [i.e., hydrostatic and osmotic pressure differences (24–26)] to the blood circulation. In adult humans, up to 8 liters per day of lymph is processed by the lymphatic system (27), of which two-thirds comes from the liver and intestines (24). Although the exact velocity ranges of this flow are unknown, measurements have suggested that they are on the order of

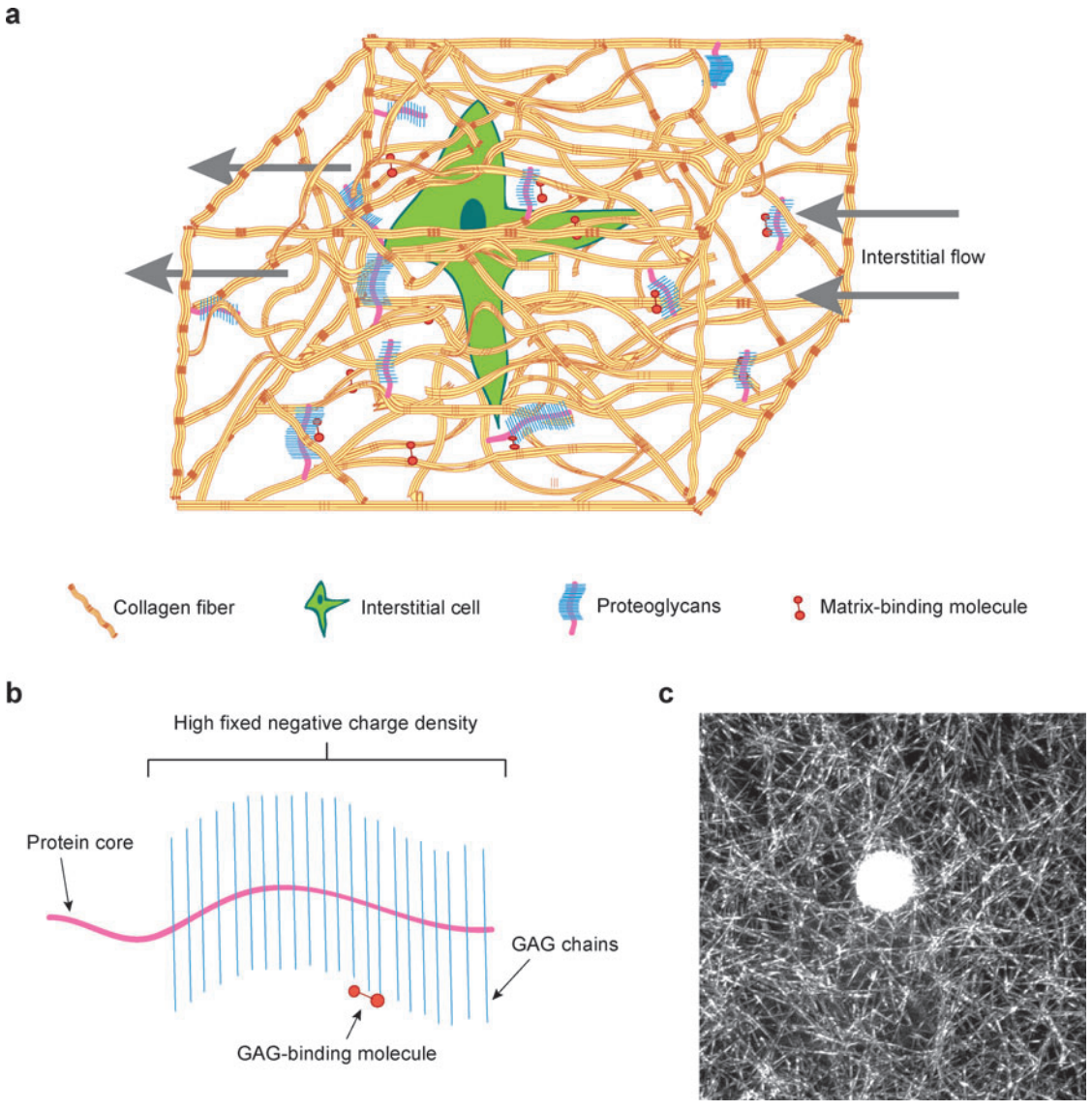

Figure 1

(*a*) Schematic of the interstitium showing major features and components of typical ECM. Here collagen fibers are intertwined along with proteoglycans and interstitial cells. (*b*) Proteoglycans (such as aggrecan and versican) are composed of a protein core and glycosaminoglycans (GAGs) side chains, such as heparin, chondroitin sulfate, and heparan sulfate, arrange like a bottle brush from the central protein core. The GAGs carry a negative charge that resists compression and fluid flow and also bind a variety of cytokines. (*c*) Confocal reflectance microscopy showing the actual fiber architecture of an in vitro fibrin gel. A 10 μm bead is shown embedded in the center.

Table 1 Major components of the interstitium

ECM component	Characteristics	Localization in body
Collagens		
I	>300-nm-long fibrils	Skin, tendon, bone, ligaments, dentin, interstitial tissues
II	>300-nm-long fibrils	Cartilage, vitreous humor
III	>300-nm-long fibrils	Skin, muscle, blood vessels
IV	Sheet forming	Basal lamina
Proteoglycans	Polysaccharides (glycosaminoglycans) attached to protein cores	Cartilage and cell surfaces, basal lamina
Fibrin	Strong fibrillar protein capable of polymerizing quickly, blood clots	Wounds and provisional matrix. Sometimes found in the tumor periphery and often used in tissue engineering
Elastin	Highly extensible protein that gives tissue elastic recoil after stretch	Blood vessels, lung, skin, and connective tissue
Laminin	Adhesive protein that glues together basal lamina	Basal lamina

0.1–2 $\mu m\ s^{-1}$ (28–30)[1], and is greatly increased during inflammation and acute edema (but not lymphedema) (24, 44, 115).

The driving forces for such interstitial, and hence lymphatic, flow are hydrostatic and osmotic pressure differences between the blood, interstitium, and lymphatics, each of which controls part of the overall lymph-forming process. Flow into the lymphatic system is driven by pressure gradients between the interstitium and lymphatic pressure, which is maintained even further negative by pumping forces in the draining lymphatic capillaries (24, 25). Local lymphatic capillary pressures are influenced by exercise, movement, and downstream integrity of the lymphatic system (24), whereas interstitial fluid pressure (IFP) results from numerous factors, including exercise, blood pressure, tissue metabolism, hydration, ECM composition, and cell density (31). For example, the integrity of the ECM is important in maintaining healthy IFP, with damage to connective components of the tissue such as collagen leading to a loss of ECM tension and subsequent change in IFP. Besides such passive structural changes, cells also play important active roles, maintaining tension in the ECM in a β1 integrin-dependent manner and therefore helping to regulate IFP (32). Measured IFPs in a variety of tissues are tabulated in Wiig et al. (33).

Although the flow of fluid between blood and lymphatic capillaries is driven by systemic pressure differences, the interstitial flow in cartilage is driven by spatially and temporally varying forces that physically compress the tissue (11, 34), as in the case of walking. This induced flow helps move nutrients, wastes, and proteins to and from chondrocytes embedded in the cartilage that may be distant from blood capillaries.

[1]It should be noted that lymph flow rates, and thus presumably interstitial flow rates, are dependent on anesthesia, and because these measurements were made in anesthetized mice, the true range of interstitial flow rates may be higher in active, awake subjects.

IFP: interstitial fluid pressure

Table 2 Properties of physiological fluids at 37°C

Fluid	Viscosity (cP)	Specific gravity	Source
Plasma	1.2	1.02	(35, 135)
Lymph	1.5–2.2	1.02	(36, 37)
Synovial fluid	10–10000	1.01	(38)
Blood	3.0–3.84	1.05	(35, 135)
DMEM	0.75–0.84	1.00	(3, 39)

The composition of the fluid that occupies the interstitial space also varies by location within the body. In most soft tissues, the source of fluid is the normal leakage of plasma from blood vessels owing to Starling forces, so unsurprisingly the interstitial fluid has a composition similar, but not identical, to that of blood plasma. Interstitial fluid contains roughly 40% of the protein concentration of plasma and exhibits a slightly altered ionic profile (24). This interstitial fluid eventually becomes lymph after entering the lymphatic system. In cartilaginous tissues one finds synovial fluid, whereas in ex vivo or in vitro tissue culture the fluid occupying the interstitium is often commercially available growth media. **Table 2** summarizes various physiological fluids that may be found in tissue interstitium and their properties, as well as DMEM, a typical culture medium, supplemented with fetal bovine serum (FBS) .

Darcy's and Brinkman's Equations

The mechanics of interstitial flow were first described by groundwater hydrologists, starting in the 1850s with Henry Darcy in Dijon, France, where his work as a municipal engineer led him to study the flow of water through the sandbeds that filtered the city's drinking water. The formula that he derived is commonly referred to as Darcy's Law:

$$\bar{v} = \frac{-K\nabla P}{\mu} \quad \text{or} \quad \bar{v} = -K' \nabla P, \tag{1}$$

where $\bar{v}$ is bulk-averaged velocity, P is pressure, μ is viscosity, and K is the specific permeability (or K' is the hydraulic conductivity).

For situations where only the mass flow rate or average velocity is needed, the Darcy equation works well. However, because it is only first order with respect to velocity, it does not permit the use of no-slip boundary conditions next to internal obstructions or bounding walls. In 1947, Brinkman proposed an additional second-order term that allowed the use of no-slip boundary conditions (40). The Brinkman equation takes the following form:

$$\nabla P = -\frac{\mu}{K}\bar{v} + \mu\nabla^2\bar{v}. \tag{2}$$

While the equation was developed heuristically, it was later proven from a statistical mechanical approach that an ensemble of particles experiencing Stokes flow results in the Brinkman equation (41–43).

Tissue Permeability and Carman-Kozeny Correlations

Permeability (K): a characteristic of a matrix that relates fluid velocity to the pressure gradient in Darcy's and Brinkman's equations

Permeability (K) depends on many factors, such as pore size, matrix composition, and matrix geometry. Furthermore, as a tissue undergoes deformation, its microarchitecture also changes, leading to variable permeability. Tissue architecture is the result of a balance between forces that want to expand tissue volume, such as osmotic pressure, hydrostatic fluid pressure, and electrostatic forces generated by GAGs, and opposing forces, such as tension in the ECM and contractile forces by cells (32). When this force balance undergoes a change, such as in the case of inflammation or edema, tissue swelling leads to microarchitectural changes and increased permeability (24). Guyton, for example, showed in an animal model that permeability varies nonlinearly with interstitial pressure, rising steeply by orders of magnitude when tissue pressure exceeded atmospheric pressure (44). Guyton, in fact, was also able to recreate this phenomenon in a nonbiological system using collapsible tubes with fibrous filling, confirming the physical basis for the pressure and swelling dependence of *K*. Similarly, increased permeability has been shown to result from lymphedema-associated tissue swelling (45, 46) and increased hydration in the cornea (16).

Alternatively, the force balance can shift in a different direction leading to tissue compaction and permeability decreases. This phenomenon can be due to externally applied forces that cause the normal architecture of fibers and matrix components to become condensed or dehydrated, such as in articular cartilage during walking (34, 48). This commonly occurs when testing tissues ex vivo (e.g., during confined compression tests) or after removing specific portions of the matrix, such as hyaluronan (47–49). During intratumoral infusions, permeability was found to vary with applied pressure, initially increasing with pressure, but ultimately decreasing by a factor of 3 to 4 from the maxima with increasing infusion pressure (50, 51); this was due, most likely, to pressure-induced local matrix compression.

Tissue permeability can be measured experimentally either in situ or ex vivo, and some examples in biological tissues and biomaterials are shown in **Table 3**. From a practical standpoint, it is often difficult to test all materials of interest, so several correlations have been developed to estimate permeability for various classes of material (52) and for biological materials (1). The relationships are based on physical and geometric idealizations of the matrix, so it is important to bear in mind that as continuum approximations they are applicable only on a macroscopic scale and do not describe the actual microscopic phenomena that are taking place in the flow (53).

The Carmen-Kozeny equation relates permeability to specific matrix properties. Several variations exist, each suited to specific geometries (54), with the general form as follows (1):

$$K = \frac{\varepsilon^3}{G\,S^2} = \frac{\varepsilon\, r_h^2}{G}, \qquad (3)$$

where ε is fractional void volume, S is the wetted surface area per unit volume, G is the Kozeny factor (related to geometry), and r_h is the mean hydraulic radius of the pores, here defined as ε/S. Because many biological matrices are composed of fibrillar components, a model assuming such a geometry is perhaps the most useful to explore.

Table 3 Selected permeabilities measured in tissues. Values are listed as either specific permeability (K) or hydraulic conductivity (K')

	Tissue/material	K (cm^2)	$K'(\frac{cm^2}{mmHg\,s} \times 10^{-8})$	Method*
Biopolymers	Fibrin coarse to fine (3 mg/ml)	10^{-8} to 10^{-11} (57)		3
	Collagen gel	10^{-12} to 10^{-14} (58)		3
	(3.5 mg/ml)	10^{-9} to 10^{-10} (13)		3
Tumors	MCaIV tumor		248 (55)	2
	LS174T tumor		45 (55)	2
	U87 tumor		65 (55) to 7000 (50)[b]	2,1
	HSTS26T tumor		9.2 (55)	2
	Rat fibrosarcoma		1.36 to1360 (51)[b]	2
	B16.F10 murine tumor		4100 to 11000 (50)[b]	1
	4T1 murine tumor		950 to 2300 (50)[b]	1
	Hepatoma		0.8 to 4.1(59)[a] 28 (1)[a]	2,1
Normal tissues	Rat abdominal muscle		15 to 78 (59)	1
	Rat dermis		5.33 (47)	2
	Mouse tail skin		70 to 150 (46)	1
	Subcutaneous plane		0.6 to 0.85 (59)[a]	1,2
	Subcutaneous slice		6 (1)[a]	2
	Vitreous body		280 to 560 (1)[a]	2
	Blood clot Unretracted/retracted	10^{-8} to 10^{-10} (57)		4
	Corneal stroma		0.7 to 1.6 (1)	2
	Mesentery		41 to 253 (1)[a]	2
	Cartilage (femoral condyle)		0.3 to 0.7 (1)[a]	2
	Cartilage (femoral head)		0.1 (1)[a]	2
	Aortic media and intima		0.4 to 2.0 (1)[a]	2
	Sclera		1.7 (1)[a]	2
	Wharton's jelly		26.7 (1)[a]	2
	Synovial intima		0.5 to 1.3 (1)[a]	1

*Method key refers to how the measurement was made: (1) in vivo, (2) ex vivo, (3) in vitro, (4) unknown.
[a]References contained within cited work.
[b]Values found to be pressure dependent.

Happel and colleagues proposed a relationship that gives the estimated flow resistance as a summation of the resistance of cylindrical fibers parallel and perpendicular to flow (52):

$$K = \frac{\varepsilon r_b^2}{k}, \tag{4a}$$

where $r_b = (s^2 - d^2)/4d$, $k = (2/3)k_+ + (1/3)k_{ll}$, s is fiber spacing, and d is fiber diameter. Orientation can affect K, with perpendicular fibers providing a larger

resistance to flow (k_+) than parallel fibers ($k_{//}$):

$$k_{//} = \frac{2\,\varepsilon^3}{(1-\varepsilon)\left[2\,\ln\left(\frac{1}{1-\varepsilon}\right) - 3 + 4(1-\varepsilon) - (1-\varepsilon)^2\right]}, \quad (4b)$$

$$k_+ = \frac{2\,\varepsilon^3}{(1-\varepsilon)\left[\ln\left(\frac{1}{1-\varepsilon}\right) - \frac{1-(1-\varepsilon)^2}{1+(1-\varepsilon)^2}\right]}. \quad (4c)$$

Porosity: the fractional volume of the extracellular matrix not occupied by solid components

From Equations 4a–c it is apparent that a given value of permeability may be realized by any number of fiber spacing/porosity combinations (53), so that permeability alone cannot fully or uniquely describe a matrix.

In biological tissues there have been many attempts to correlate permeability to specific components, such as collagen or GAGs (55). This approach is overly simplistic and does not consider the role, for example, that even a small quantity of GAGs in a primarily collagenous tissue plays to maintain matrix architecture (49). Levick (1) showed that matrix permeability is a combination of the drag effects of both collagen fibers and GAGs, essentially confirming the assumption made in the more general permeability correlations listed above, i.e., that all physical species that occlude flow, whether fibrous or not, contribute to the overall resistive effect of the matrix. The role of fixed charges on matrix components is to increase the size of the immobile water layer that associates with the component, effectively giving the charged component a larger surface area. An approach correlating matrix surface area to permeability has been demonstrated in ocular tissue by converting information from micrographs into specific surface area and porosity information, which, using Equation 3, yielded permeabilities that were in general agreement with the experiment (56).

Interstitial Velocity Profiles Around Cells

Darcy's law is a continuum approximation of the actual microscopic flow phenomena that occurs in a porous media. In essence it represents the most zoomed-out view of events. For example, it cannot give information on flow profiles between fibers or around cells. The Brinkman equation, on the other hand, allows for velocity fluctuations around solid bodies in the flow field, such as a no-slip boundary on the surface of a cell embedded in a porous matrix, but the porous medium itself, e.g., the individual fibers, is still "invisible" and treated as a continuum. If one instead considered all of the individual fibers and the adhesion complexes that bind the cell body to these fibers, one could return to Navier-Stokes as the governing fluid dynamics equation because it would be unnecessary to make averaging assumptions for the fibers because their location and dimensions would be exactly known. In solving the real flow field at the cell surface, one would see a locally discontinuous and inhomogeneous flow field owing to the fibers that would be significantly different than that predicted by the solution of Brinkman's equation (**Figure 2**).

At the cellular level it is speculated that shear stress due to interstitial flow is "felt" by the cell using individual molecules or adhesion plaques, which would be on the same size scale or smaller than the actual flow discontinuities. This shows an important limitation of using an approximation such as that assumed with Brinkman's equation. Furthermore, local cellular modification, such as alignment or local

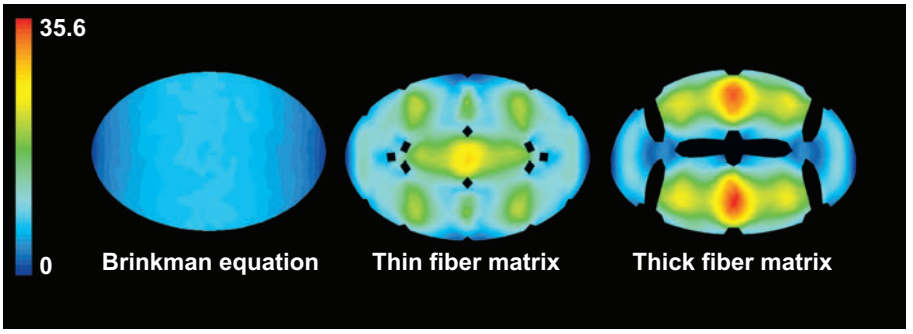

Figure 2

Continuum approximations such as Darcy's law for flow through porous medium fail to capture microscopic variations in shear stress through the matrix. The three images show computed shear stress on a cell surface under low Reynolds number interstitial flow, with pseudocolor indicating relative magnitude (*red* = maximum, *blue* = minimum). The result on the left was computed from the Brinkman equation, and the two on the right were calculated using the Navier Stokes equation, assuming explicit fiber sizing and spacing. In all three cases the permeability value was the same, but the Navier Stokes solutions reveals the range in shear stress on the cell surface and predicts much larger shear stresses than estimated by the Brinkman approximation, depending on the details of fiber diameter and spacing. Figure reprinted from Reference 53 with permission from Elsevier.

(pericellular) matrix fiber contraction by interstitial cells, has the potential to significantly shield the cell from environmental stresses (53). One could argue then against the use of continuum approximations, but given a lack of precise spatial and geometric information about every fiber in a tissue (see **Figure 1*c***) and the obvious computational expenditure that would be required even if this information were known, it becomes clear why continuum approximations such as Darcy and Brinkman's laws are used.

INTERSTITIAL MASS TRANSPORT

Mass transport within the interstitium is critical for the maintenance of interstitial cells. Solute transport within the space between blood capillaries, which ranges in size from several hundred microns in soft tissue (25, 60, 61) to several millimeters in the case of cartilage (11), is facilitated by both convection and diffusion according to the general mass transport balance,

$$\frac{\partial C_i}{\partial t} + \underline{u}_i \cdot \nabla C_i = D_{ij}\nabla^2 C_i + R_i, \qquad (5)$$

where $\underline{u}_i$ is the solute velocity vector; C_i is the concentration of the solute of interest; D_{ij} is the diffusion coefficient of the solute in solvent j (here assumed to be isotropic); $\nabla^2$is the Laplacian operator; R_i is the reaction rate that accounts for consumption, degradation, generation, or binding of species i to the matrix (see **Figure 3**); and t is time. Typically, because interstitial flow rates are quite small, the convective portion of Equation 5 is often simply ignored. Caution must be exercised, however, in neglecting convection (even at low Peclet numbers), as discussed in the next section.

Peclet number (*Pe*): dimensionless ratio of convective to diffusive contributions to mass transfer. $Pe = Lu_i/D_{ij}$

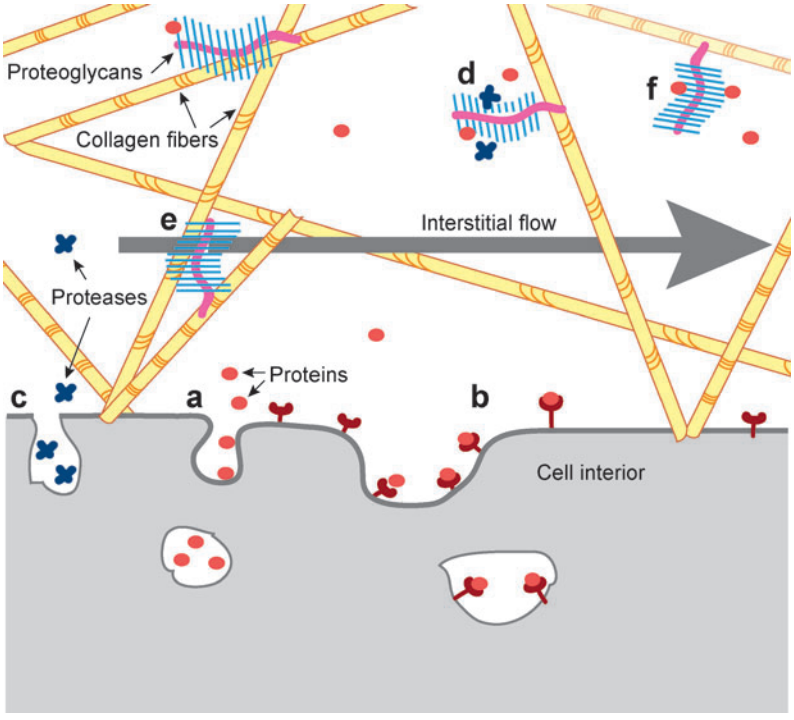

Figure 3

A microscopic view of the ECM-cell interface reveals the many events that play a role in interstitial transport. Cells actively participate in the mass transport process by (*a*) secreting proteins (*sphere*), (*b*) binding and internalizing proteins, and by (*c*) releasing proteases (*x*) that can (*d*) liberate ECM-bound proteins. The ECM components (*e*) provide resistance to convection and diffusion as well as (*f*) serving as a storage site for ECM-binding proteins.

Diffusion Coefficient Correlations

In a dilute isotropic solution, the diffusion coefficient of a large solute molecule can be estimated using the Stokes-Einstein equation:

$$D_{ij} = \frac{k_B T}{6\pi \mu_j r_i}, \tag{6}$$

where k_B is Boltzmann's constant, T is temperature, μ_j is viscosity of solvent j, and r_i is molecular radius or effective hydrodynamic radius. In practice this equation is often employed to estimate the hydrodynamic radius by experimentally determining the diffusion coefficients using a method such as fluorescence recovery after photobleaching (FRAP). Alternatively, several correlations have been developed specifically for proteins, notably that of Berk (62), $D_o = 3600(MW)^{-0.34}$, which is valid at 23°C, or of Young (63), where $D_{ij} = 8.34(\frac{T}{\mu_j MW_i^{1/3}})$, which essentially reduces to the Berk relation when considering a fluid with the ratio of temperature (in K) to viscosity (cP) of approximately 203.

These correlations assume that diffusion occurs in free solution, while in real tissues or in vitro matrices steric restrictions owing to pore size, as well as ionic interactions between solutes and certain matrix components, can reduce diffusivities to 18 to 93% of their free solution value (62, 64–66). Several relationships exist to calculate the expected diffusion coefficient of a solute in a porous material if the coefficient is known in free solution. Ogston (67) was among the first to propose a

model for the relationship between the free and matrix diffusivity with the following form:

$$\frac{D}{D_o} = A \exp(-b\, r\, c^{0.5}), \tag{7}$$

where A is a dimensionless constant with a value between 1 and 2 (often assumed 1), b is a dimensionless constant (taken by Ogston to be π), r is the solute radius, and c is a matrix concentration term expressed as length of matrix fiber per volume. This relation was further modified by Kosto & Deen (68) to account for fiber radius, which in the Ogston relationship is assumed to be zero:

$$\frac{D_G}{D_o} = \exp(-\phi^{0.5}\,(1 + R_H/r_f)), \tag{8}$$

where ϕ is fiber volume fraction, R_H is the hydrodynamic radius of the pores, and r_f is the fiber radius. Other models have been developed that calculate the effect of the matrix on diffusivity as a product of steric (S) and hydrodynamic (F) effects (69, 70) in the form $D = SF D_o$, where D_o is the diffusion coefficient in free solution, F is a function of K, and r_s, and S is a function of the volume fraction of fibers.

$$F = 1 + \frac{r_s}{\sqrt{K}} + \frac{1}{9}\left(\frac{r_s}{\sqrt{K}}\right)^2 \tag{9a}$$

and

$$S(f) = e^{-0.84 f^{1.09}}, \tag{9b}$$

where $f = (1 + \frac{r_s}{r_f})^2 \phi$.

Alternatively, some literature values of diffusion coefficients for certain protein-matrix pairs exist (**Table 4**). Although the odds of finding the solute/matrix pair of interest are low, the diffusivity of a solute in one matrix can be converted to diffusivity

Table 4 Measured diffusivities in physiological tissues and biological matrices

Solute	Diffusivity ($\mu m^2\ s^{-1}$)	Tissue type (Reference)
70 k Dextran	20–40	Cartilage (73)
	100–200	Fibrin (11%–7%) (74)
	250	Alginate (2%) (74)
10 K Dextran	5–20	Cartilage (50% and 10% compression) (75)
IgG	5.4–31.2	Excised tumors (55)
	1–100	Collagen (4.5%–1%) (65)
IgM	7.68–41.6	Excised tumors (71)
BSA	39–70	Rabbit ear (28)
	40–88	Neoplastic rabbit ear (28)
	56.6–113	Human colon adenocarcinoma (71)
	11.9	LS174T tumor (71)
Oregon Green	5–30	Cartilage (50% and 10% compression) (75)

in another matrix using the relationship suggested by Kosto & Deen (68):

$$\frac{D_{i1}}{D_{i2}} = \frac{S_2\left(1+\left(\frac{r_s}{\sqrt{K_2}}\right)+\frac{1}{9}\left(\frac{r_s}{\sqrt{K_2}}\right)^2\right)}{S_1\left(1+\left(\frac{r_s}{\sqrt{K_1}}\right)+\frac{1}{9}\left(\frac{r_s}{\sqrt{K_1}}\right)^2\right)} \quad (10)$$

Morphogen: any bioactive molecule capable of eliciting cell response such as migration, organization, or differentiation

Here S represents a steric function as in Equation 9, but the ratio of S values for two different matrices is often assumed to be unity. Finally, it is also possible to conduct FRAP experiments for the specific protein/matrix pair of interest (62, 71). It should be noted that all of these models allow the estimation of an "effective" diffusivity but implicitly assume static conditions. When convection is present, the tortuous path that the fluid must take around matrix fibers has a dispersive effect, and this contribution to diffusion can also be estimated from empirical correlations (72).

Convective Solute Transport

Even though interstitial velocities may be small, the role of convection in the overall distribution of proteins can be significant. Diffusion is inversely related to molecular size and many biologically significant proteins, pharmaceuticals, and delivery vectors are quite large, leading to small diffusion distances over biologically relevant timescales. Convection, however, is only weakly tied to molecular size (as long as the molecular size does not result in entrapment within the ECM), which means that for larger molecules, convection becomes more important in governing their transport compared to diffusion. The Peclet number (*Pe*) is a dimensionless ratio of the relative contributions of convection and diffusion to transport: $Pe = Lu_i/D_i$, where u_i is the bulk convective velocity of the solute i, D_i is its diffusion coefficient, and L is a characteristic length (e.g., when concerned with cell morphogenetic phenomena it might be the cell radius).

The Peclet number is typically the metric used to decide whether convection can be neglected. An important nuance in this decision-making process centers on the underlying motivation for modeling the mass transfer. When the only concern is solute penetration depth, convection can be safely ignored in low *Pe* cases. Convection cannot be ignored, however, in modeling local solute distributions, such as in morphogenic events, where morphogen gradients across a cell as small as 1% have been shown to trigger cell response (76). Indeed, small but physiological Peclet numbers can lead to gradients in morphogens (77) that have the potential to guide morphogenesis. In such cases, ignoring the small convective contribution leads to the complete loss of such subtle influences of convection.

The use of Equation 5 requires that the solute velocity profile, $\underline{u}_i$, which is related (or equal) to the fluid velocity profile, be known. This can be solved simultaneously using the Brinkman equation (Equation 2), but except for a few limiting cases (78, 79), solving Equation 5 requires the use of computational techniques. Commercially available packages such as FLUENT (Fluent Inc., Lebanon, NH) or COMSOL (COMSOL AB, Stockholm, Sweden) have coupled momentum and mass transfer capabilities that can handle most problems.

In modeling convective solute transport in porous matrices, the pore size distribution can hinder or enhance solute convective velocity relative to that of the fluid. For example, if the matrix creates steric hindrance or if charge interactions between the solute and the matrix effectively slow the molecular transport, the mean solute convective velocity $\underline{u}_i$ may be smaller than that of the solvent $\underline{v}$ (80, 81). However, if the matrix charge repels the solute or if the solute is large enough so that it can access only the larger pores, size exclusion effects can be seen where the solute travels with only the faster fluid velocities and then $\underline{u}_i > \underline{v}$. Therefore, although steric effects of the matrix can slow the diffusion velocities of proteins, they can at the same time enhance convective velocities (82–84). A convection coefficient φ_i is sometimes used to relate solute and solvent velocity linearly, and again, this coefficient may be greater or less than 1:

$$\underline{u}_i = \varphi_i \underline{v} \tag{11}$$

Beyond a certain size, however, steric hindrance of proteins or particles can eventually cause complete entrapped in the matrix (83, 85, 86), an important limitation in the construction of microcarrier-based drug delivery therapies.

BIOLOGICAL MODELS OF TRANSPORT

Solute-Matrix Interactions

While the ECM provides a structural support for cells and modulates physical forces, it also takes on an active role in protein storage, trafficking, and processing. The individual components of the ECM, such as collagen, fibrin, and proteoglycans, present unique biochemical interfaces for the interstitial fluid and associated proteins that pass through the ECM. Many extracellular signaling proteins (herein referred to generically as morphogens) have specific binding motifs for these ECM components (particularly sulfated proteoglycans) leading to accumulation of bound morphogen stores in the ECM. Examples include VEGF, basic FGF, TGF-β, CCL21, and many others (**Table 5**). Alternatively, biomaterials scientists have engineered this functional feature of the ECM with matrix-binding protein variants or peptides (reviewed in Reference 23).

Evidence has shown that cells actively make use of these matrix-bound morphogen stores (95–97), giving them more nuanced methods of actively modifying their environment. While adding flexibility from the cell's perspective, matrix-binding characteristics of morphogens add complexity to the cell biologist's quest to understand specific morphogenetic cell responses. The traditional paradigm of measuring cell response to various morphogens by culturing cells on plastic and adding predetermined amounts of these cytokines to develop dose-response curves fails to account for the differences in signaling between bound versus free morphogens, as well as spatial differences around the cell in signaling molecules made possible by a 3-D matrix. Indeed, several studies have shown markedly different response patterns to bound morphogens in three dimensions when compared to two dimensions (97, 98). Therefore, when considering a paradigm where the ECM is also part of the overall

Table 5 Selected matrix binding morphogens and proteases (adapted from Reference 77)

Morphogen or chemokine	Molecular mass (kDa)	Binding substrate	Cellular effect
VEGF165	38.2 (dimer)	Proteoglycans (87, 89) Fibrin (99)	Vascular permeabilityand angiogenesis
bFGF	18	Fibrin (92, 99) GAGs (89, 90)	Upregulation of u-PA, u-PAR, and u-PAI
CCL5 CCL17 CCL21	7.5–14	Sulfated GAGs (93, 94)	Leukocyte recruitment
Interleukin-1B	17	Fibrin (98)	Upregulation of NO and chemokines
VonWillebrand Factor	20	Fibrin (100) Collagens and glycoproteins (134)	Platelet adhesion and storage of factor VIII
Endostatin	20	GAGs (101)	Angiogenesis inhibitor
PEDF	50	GAGs/collagen (102)	Neurotrophic and antiangiogenic
Protease	**Molecular mass (kDa)**	**Specificity**	
u-PA	31–50	Plasminogen	
t-PA	70	Plasminogen	
Plasmin	92	Fibrin	
MMP2	64–72	Collagen/gelatin	
MMP3	43–52	Fibrin collagen/gelatin	
MMP9	84–92	Collagen	
Sulf-2	72	Heparin and heparan sulfate (88)	

signaling mechanism, the actual chemical makeup of the matrix matters to protein transport as much as its geometrical considerations such as porosity and permeability.

In the context of modeling mass transport as discussed above, the binding, storage, and release of morphogens can be accounted for in a reaction term R_i, which depends on the binding behavior of the particular solute. For example, for a simple noncompeting 1:1 binding reaction, R_i could take the following form:

$$R_{Morphogen} = -k_{on} C_{Morpb} C_{BS} + k_{off} C_{BS-Morpb}, \quad (12)$$

where k_{on} and k_{off} are rate constants specific for the morphogen/binding site pair, C_{Morpb} is the concentration of morphogen, C_{BS} is the concentration of binding sites, and $C_{BS\text{-}Morpb}$ is the concentration of bound morphogen. The relative affinity of a substrate is often indicated by its K_d ($= k_{off}/k_{on}$).

The Role of the Cell in Mass Transport

Thus far, the diffusion, convection, and binding of morphogens in and through porous ECM have been discussed, but without considering active mechanisms by cells that influence morphogen distributions. Cells secrete, bind, release, and respond to

MMP: matrix metalloproteinase

morphogens, and a typical goal for the bioengineer is the control or quantification of growth, differentiation, and organization of cells. A mathematical solution of the governing equations requires knowledge of this active role taken by the cells (**Figure 3**).

Specifically, while morphogen-matrix binding can occur in the absence of cells and is governed by an equilibrium binding constant K_d, this equilibrium can be shifted by cell-secreted enzymes, such as matrix metalloproteinases (MMPs), plasmin, and sulfatases as well as by competing matrix-binding molecules if the concentration of matrix binding sites is relatively low. Heparanase, for example, has now been implicated in the vascularization and metastasis of tumors (103–105), with the action of this enzyme tied not only to its ability to physically degrade matrix but also to its ability to release bound growth factors such as VEGF and bFGF (106). The various other enzymes work on specific matrix components and morphogens by different mechanisms such as denaturing binding sites (88), cleaving a portion of the bound morphogen (97), or cleaving the binding molecule itself, leaving a soluble morphogen with a portion of the binding molecule still attached (106–108). Regardless of the specific mechanism, this release can also be accounted for in the R_i term of Equation 5 if sufficient information regarding the mechanism is known.

If one wants to take into consideration the secretion, binding, and trafficking of proteins at the cell surface in terms of modeling interstitial transport, the cell can be used as a boundary condition (for microscale models) or as part of the continuum for more macroscale models. Internal cell signaling and secretory systems are very complex and highly regulated systems for which many models have been created. Including such an internal cell-signaling model into an extracellular transport model is possible, but frequently the complexity of these systems is simplified to either a constant flux or concentration boundary assumption. The mechanisms regulating cell surface signaling and secretion can alternately be probed using mathematical methods in a recursive manner (109–111). In this way, proposed mechanisms can be modeled to predict macroscopic responses. Such computational analyses can provide insight into the microscopic cell surface phenomena that would be otherwise difficult to probe experimentally.

Coupled Models

The Brinkman and Darcy equations were formulated with a fixed or rigid solid (porous) phase in mind, but of course, tissues can deform and compress with movement and localized changes in pressure and therefore the ECM porosity and conductivity can be a function of fluid pressure or solid stress. To account for such interactions, Darcy's law can be coupled into a constitutive model of stress-strain behavior to relate overall matrix strain with fluid pressure and flow. Such poroelastic or biphasic models are useful for describing tissue swelling (46, 112) or matrix compression, as in cartilage and bone (12, 34, 113). Furthermore, these models can be incorporated to estimate solute transport in deforming tissues (84, 114).

Interstitial mass and fluid transport in tissues is often intimately tied not only to the properties of the interstitium but also to the sources and sinks of interstitial

fluid. Appropriate treatment of such cases involves including each stage of the transport process either in a compartmentalized or integrated model. Models that integrate transport between blood, interstitium, and lymphatic compartments—on a macroscale using Starling's Law—are among the earliest work describing tissue transport (115, 116). Lymphedema, for example, is a disease where lymph drainage is decreased and interstitial fluid accumulates in interstitial spaces to cause chronic swelling. This is very different from acute edema due to inflammation, where the lymphatic vessels function properly and interstitial flow can be quite high compared with normal conditions, but the tissue swells due to matrix breakdown and increased compliance. The most common type of lymphedema is caused by damage to larger lymphatic vessels or nodes owing to radiation or lymph node removal in cancer, or blockage of lymphatics as in filariasis. In this case the fluid movement stops in the interstitium despite adequate transport properties (i.e., permeability) because there is no net driving force for fluid drainage.

EPR: enhanced permeability and retention

SIGNIFICANCE

Role of Interstitial Transport in Delivery of Drugs and Therapeutics

Much of the applied research into interstitial transport to date has been driven by the desire to understand transport limitations encountered in delivering therapeutics to targeted tissues such as tumors. The pharmaceutical industry has traditionally bypassed these transport limitations with small-molecule therapeutics with high diffusivities, delivered systemically. However, as new therapeutic research is increasingly focused on large molecules and delivery vehicles, transport issues become critical challenges. In particular, protein and antibody therapies and synthetic drug carriers (including retroviruses, nanoparticles, microsomes and liposomes, etc.) are emerging that can be inhaled, injected, or released from an intracorporeal device. With these new drug technologies come an increasing importance of interstitial transport issues.

Tumors are a common target of carrier-based drugs because of their obvious pathological nature and their unique mass transport properties. Tumors often have leaky vessels and nonfunctional internal lymphatics (30), which in turn leads to exudation and accumulation of large quantities of macromolecules, a phenomenon known as enhanced permeability and retention (EPR) (117, 118). Although the large size of an agent can aid in the retention of such large therapeutics in tumors, once exuded from the vascular system, interstitial transport becomes the limiting factor to effective intratumoral distribution (30, 119). The high interstitial fluid pressure that is typical within tumors leads to a decreased convective driving force across the vessel wall and also a decrease in pressure variation within the tumor mass itself (120), therefore hampering both drug distribution internal to the tumor as well as drug delivery from the periphery into the tumor mass. A second limiting factor to interstitial transport is the often reduced mobility of the delivery vehicles because of steric effects. Reduced pore size and/or matrix-molecule interactions combine to "trap" molecules in the region just around the vascular source (86, 117, 121). The effect is that the convection coefficient φ_i in Equation 11 and the diffusivity ratio of Equation 8 are both substantially

decreased. It has been suggested that enzymes such as collagenase and hyaluronidase could be used to disrupt the tumor ECM and render it more amenable to interstitial transport, and experiments have shown increased permeability, diffusivity, improved IFP profiles, and increased penetration and uptake of test molecules with such enzyme treatments (55, 120, 122). The clinical relevance of such treatments is still unclear, however, as disruption of the tumor ECM not only allows easier interstitial transport of potential therapeutics, but it also lowers the barriers to tumor cell metastasis (123, 124).

The interstitial-lymphatic transport route can also be exploited for drug delivery, particularly for targeting immune cells in lymph nodes (125). Nanoparticles can be constructed to present specific antigens to dendritic cells and subsequent cascade, resulting in the activation of T cells. This mechanism, however, depends on delivery of the nanoparticles to the lymphatic system, where much of the immunological function resides. The efficacy of the immune response is dependent on the control of the spatial and temporal presentation of antigens, which is ultimately dictated by interstitial transport and the lymphatic system (85). Delivery of nanoparticles to the lymphatic system is usually via interstitial injection, thus interstitial transport considerations are paramount to the success of such methodology.

Interstitial Transport as a Central Theme in Developmental Biology

Interstitial transport of proteins plays a critical role in morphogenesis because cells respond to very small gradients of morphogens to direct their differentiation and development into tissues and organs. The seminal work of Alan Turing in 1952 (126) sought to describe how complex biological patterns such as those seen in flower petals and seashells use fairly simple transport models of diffusive mass transfer and chemical reactions. Since then, analytical and computational models of morphogenesis have continued to focus on diffusion and reaction without considering the importance of convection. However, recent studies have demonstrated that fluid convection may indeed play a critical role in morphogenesis, notably with the work of Nonaka and colleagues (18). They showed that exquisitely small localized convective flows of amniotic fluid around a mouse embryo caused by the cilial node were responsible for the normal left-right asymmetric development of the embryo resulting in, for example, the placement of the heart. When the direction of flow was reversed, so was the location of the heart and other asymmetric organs. While the mechanisms remain unknown, this phenomenon has been well studied in recent years (133).

How Do Cells "Sense" Interstitial Flow?

It is now relatively well established that interstitial flow can induce morphogenic effects in cells beyond simply that of enhancing nutrient transport to otherwise nutrient-poor areas. Specific examples of the morphogenic effects of interstitial flow include lymphatic regeneration in a wound-healing model, whereby lymphatic regeneration occurred in the direction of flow (7); when this flow was severely decreased, architecture and function did not return (8). Another example is the demonstration

that cyclic compression and corresponding convection caused biased deposition of newly synthesized ECM matrix deposition in cartilage (127). In vitro, the morphogenic influence of interstitial flow has been shown in capillary morphogenesis (3, 5, 6), cytokine production in smooth muscle cells (15), and fibroblast alignment and differentiation (13, 128).

Autologous chemotaxis: the ability of a cell to both produce and follow its own chemotactic gradient. This is facilitated by flow and matrix interactions

Despite these findings, the mechanisms whereby cells sense slow interstitial flow have not been well established, although shear stresses have been estimated (53, 129). It is possible that any of the well-studied mechanotransduction mechanisms—including stretch-activated ion channels, activation of adhesion complexes by tensile strain, and membrane shear (reviewed in Reference 130)—may be responsible. It is also probable that dynamic matrix strain or interstitial fluid flow may cause changes in the extracellular distribution of signaling proteins, which in turn may drive cell response, particularly because cells get directional cues by the local concentration gradients of chemokines and growth factors that exist in the pericellular milieu. However, this mechanotransduction mechanism is difficult to prove experimentally because mechanical stress and extracellular protein distributions are inherently coupled. Still, a few recent studies have explored this mechanism by combining computational with in vitro experiments. Helm et al. (3) showed that although interstitial flow and a matrix-bound growth factor individually had a small effect on capillary morphogenesis, the combined cues showed a synergistic effect that could be explained by increased and directional liberation (activation) of the growth factor according to computational modeling (77): Through the combined action of convective transport, matrix binding of morphogen, and proteolytic release of bound morphogen stores, the pericellular gradient was sufficiently asymmetric to be within sensing range of the cell (**Figure 4**). Two other studies have explored the temporal variation of autocrine ligands owing to tissue compression, and they have concluded that cells can sense changes in their mechanical environment owing to time-varying changes in pericellular ligand concentrations (111, 131).

A more direct demonstration of interstitial flow-induced morphogen redistribution has been recently shown with autologous chemotaxis of tumor cells via signaling through the chemokine receptor CCR7. Although slow flow induced directional migration, CCR7 blocking could inhibit this response, and thus it was truly a chemotactic response but was caused by autocrine CCR7 ligand secretion and interstitial flow (132). This is significant for cell homing to lymph nodes, which is critical for both dendritic cell activation of T cells and tumor cell metastasis because interstitial flow is always directed toward functional lymphatic vessels. Although autologous and flow-enhanced paracrine chemotaxis of tumor cells or dendritic cells has not yet been proven in vivo, the implications are that the dynamic forces involved in the local interstitial transport around tumors could play an important role in metastasis via the lymphatic system.

Outlook

As biomedical engineers continue to work toward the realization of cultured replacement organs, the challenges to understanding and recreating physiological conditions

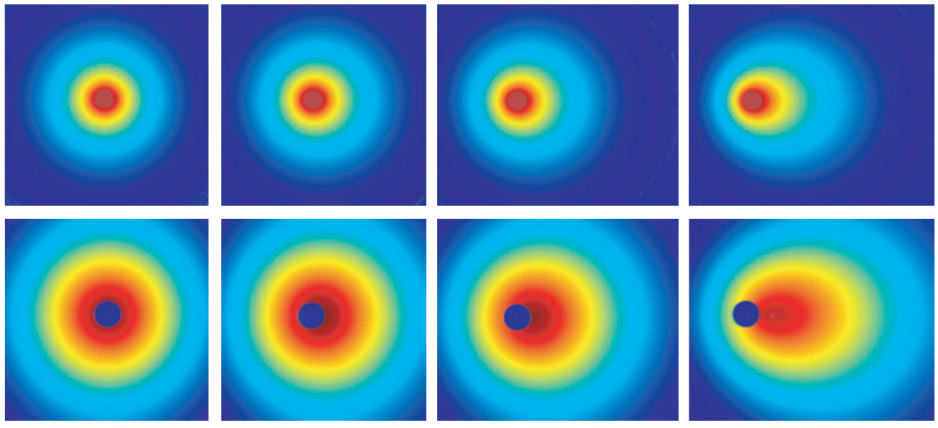

Velocity μm/s	0	0.6	1.2	3.0
Cell-released gradient %	0	1	1	3
ECM-released gradient %	0	11	23	62

Figure 4

Autologous gradient formation is made possible by flow and matrix interactions. Two-dimensional simulations compare the pericellular gradients of a cell-secreted protein with $D_{ij} = 120\ \mu m^2/s$ around a 20 μm cell (*top row*) with the same morphogen when it is released from the matrix owing to cell-released proteases (*bottom row*) under various flow conditions. Figure adapted from Reference 77.

remain significant. As understanding of cellular behavior evolves, it has become clear that cellular response is seldom tied to one individual input, but rather an intersecting array of inputs. In efforts to recreate physiological phenomena, however, this complex network environment of biophysical and biochemical factors has been often oversimplified to one factor only, as in efforts to promote certain behaviors such as growth and/or angiogenesis. It is now becoming increasingly clear that biochemical signaling depends on the mechanical environment, i.e., 3-D matrices and interstitial flow, and that biophysical and biochemical signaling are intertwined. The future success of tissue engineering, advanced targeted drug delivery, and even the continued elucidation of biological processes such as morphogenesis requires an increasingly interdisciplinary approach coupling biology with transport considerations.

DISCLOSURE STATEMENT

The authors are not aware of any biases that might be perceived as affecting the objectivity of this review.

ACKNOWLEDGMENTS

The authors would like to thank John Pedersen and Joseph Rutkowski for valuable suggestions during manuscript preparation. Financial support to M.A.S. was provided by the Swiss National Science Foundation, the NIH-NHLBI, and the U.S. National Science Foundation.

LITERATURE CITED

1. Levick JR. 1987. Flow through interstitium and other fibrous matrices. *Q. J. Exp. Phys.* 72:409–37
2. Cukierman E, Pankov R, Stevens DR, Yamada KM. 2001. Taking cell-matrix adhesions to the third dimension. *Science* 294:1708–12
3. Helm CLE, Fleury ME, Zisch AH, Boschetti F, Swartz MA. 2005. Synergy between interstitial flow and VEGF directs capillary morphogenesis in vitro through a gradient amplification mechanism. *Proc. Natl. Acad. Sci. USA* 102:15779–84
4. Helm CLE, Zisch AH, Swartz MA. 2006. Engineered blood and lymphatic capillaries in 3D VEGF-fibrin-collagen matrices with interstitial flow. *Biotech. Bioeng.* 96(1):167–76
5. Ng CP, Helm CLE, Swartz MA. 2004. Interstitial flow differentially stimulates blood and lymphatic endothelial cell morphogenesis in vitro. *Microvasc. Res.* 68:258–64
6. Semino CE, Kamm RD, Lauffenburger DA. 2006. Autocrine EGF receptor activation mediates endothelial cell migration and vascular morphogenesis induced by VEGF under interstitial flow. *Exp. Cell Res.* 312:289–98
7. Boardman KC, Swartz MA. 2003. Interstitial flow as a guide for lymphangiogenesis. *Circ. Res.* 92(7):801–8
8. Rutkowski JM, Boardman KC, Swartz MA. 2006. Characterization of lymphangiogenesis in a model of adult skin regeneration. *Am. J. Physiol. Heart Circ. Physiol.* 291:H1402–10
9. Buschmann MD, Gluzband YA, Grodzinsky AJ, Hunziker EB. 1995. Mechanical compression modulates matrix biosynthesis in chondrocyte agarose culture. *J. Cell Sci.* 108:1497–508
10. Maroudas A, Bullough P, Swanson SAV, Freeman MAR. 1968. The permeability of articluar cartilage. *J. Bone Joint Surg.* 50B:166–77
11. Mow VC, Holmes MH, Lai WM. 1984. Fluid transport and mechanical-properties of articular-cartilage—a review. *J. Biomech.* 17:377–94
12. Grodzinsky AJ, Levenston ME, Jin M, Frank EH. 2000. Cartilage tissue remodeling in response to mechanical forces. *Annu. Rev. Biomed. Eng.* 2:691–713
13. Ng CP, Swartz MA. 2003. Fibroblast alignment under interstitial fluid flow using a novel 3-D tissue culture model. *Am. J. Physiol. Heart Circ. Physiol.* 284:H1771–77
14. Ng CP, Swartz MA. 2006. Mechanisms of interstitial flow-induced remodeling of fibroblast-collagen cultures. *Ann. Biomed. Eng.* 34:446–54

15. Wang S, Tarbell JM. 2000. Effect of fluid flow on smooth muscle cells in a 3-dimensional collagen gel model. *Arterioscl. Thromb. Vas.* 20:2220–25
16. Ethier CR, Johnson M, Ruberti J. 2004. Ocular biomechanics and biotransport. *Annu. Rev Biomed. Eng.* 6:249–73
17. Powers MJ, Domansky K, Kaazempur-Mofrad MR, Kalezi A, Capitano A, et al. 2002. A microfabricated array bioreactor for perfused 3D liver culture. *Biotech. Bioeng.* 78:257–69
18. Nonaka S, Tanaka Y, Okada Y, Takeda S, Harada A, et al. 1998. Randomization of left-right asymmetry due to loss of nodal cilia generating leftward flow of extraembryonic fluid in mice lacking KIF3B motor protein. *Cell* 95:829–37
19. Nagy JA, Brown LF, Senger DR, Lanir N, Van de Water L, et al. 1989. Pathogenesis of tumor stroma generation—a critical role for leaky blood-vessels and fibrin deposition. *Biochim. Biophys. Acta* 948:305–26
20. Griffith LG, Swartz MA. 2006. Capturing complex 3D tissue physiology in vitro. *Nat. Rev. Mol. Cell Biol.* 7:211–24
21. Lutolf MP, Hubbell JA. 2003. Synthesis and physicochemical characterization of end-linked poly(ethylene glycol)-copeptide hydrogels formed by Michael-type addition. *Biomacromolecules* 4:713–22
22. Langer R, Tirrell DA. 2004. Designing materials for biology and medicine. *Nature* 428:487–92
23. Lutolf MP, Hubbell JA. 2005. Synthetic biomaterials as instructive extracellular microenvironments for morphogenesis in tissue engineering. *Nat. Biotech.* 23:47–55
24. Guyton AC. 1991. *Textbook of Medical Physiology*. Philadelphia: Saunders
25. Schmid-Schonbein GW. 1990. Microlymphatics and lymph-flow. *Phys. Rev.* 70:987–1028
26. Swartz MA. 2001. The physiology of the lymphatic system. *Adv. Drug Del. Rev.* 50:3–20
27. Renkin EM. 1986. Some consequences of capillary-permeability to macromolecules—starlings hypothesis reconsidered. *Am. J. Physiol. Heart Circ. Physiol.* 250:H706–10
28. Chary SR, Jain RK. 1989. Direct measurement of interstitial convection and diffusion of albumin in normal and neoplastic tissues by fluorescence photobleaching. *Proc. Natl. Acad. Sci. USA* 86:5385–89
29. Dafni H, Israely T, Bhujwalla ZM, Benjamin LE, Neeman M. 2002. Overexpression of vascular endothelial growth factor 165 drives peritumor interstitial convection and induces lymphatic drain: magnetic resonance imaging, confocal microscopy, and histological tracking of triple-labeled albumin. *Cancer Res.* 62:6731–39
30. Jain RK. 1999. Transport of molecules, particles, and cells in solid tumors. *Annu. Rev. Biomed. Eng.* 1:241–63
31. Aukland K, Reed RK. 1993. Interstitial-lymphatic mechanisms in the control of extracellular fluid volume. *Physiol. Rev.* 73:1–78
32. Reed RK, Rubin K, Wiig H, Rodt SA. 1992. Blockade of beta(1)-integrins in skin causes edema through lowering of interstitial fluid pressure. *Circ. Res.* 71:978–83

33. Wiig H, Rubin K, Reed RK. 2003. New and active role of the interstitium in control of interstitial fluid pressure: potential therapeutic consequences. *Acta Anaesth. Scand.* 47:111–21
34. Kwan MK, Lai WM, Mow VC. 1984. Fundamentals of fluid transport through cartilage in compression. *Ann. Biomed. Eng.* 12:537–58
35. Fournier RL. 1998. *Basic Transport Phenomena in Biomedical Engineering*. Philadelphia: Taylor and Francis. 312 pp.
36. Dixon J, Greiner S, Gashev A, Cote G, Moore JJ, Zawieja D. 2006. Lymph flow, shear stress, and lymphocyte velocity in rat mesenteric prenodal lymphatics. *Microcirculation* 13:597–610
37. Burton-Opitz R, Nemser R. 1917. The viscosity of lymph. *Am. J. Physiol.* 45:25–29
38. Mazzucco D, McKinley G, Scott RD, Spector M. 2002. Rheology of joint fluid in total knee arthroplasty patients. *J. Orthop. Res.* 20:1157–63
39. Gosgnach W, Messika-Zeitoun D, Gonzalez W, Philipe M, Michel JB. 2000. Shear stress induces iNOS expression in cultured smooth muscle cells: Role of oxidative stress. *Am. J. Physio. Cell Physiol.* 279:C1880–88
40. Brinkman HC. 1947. A calculation of the viscous force exerted by a flowing fluid on a dense swarm of particles. *App. Sci. Res. A Mech.* 1:27–34
41. Durlofsky L, Brady JF. 1987. Analysis of the brinkman equation as a model for flow in porous media. *Phys. Fluids* 30:3329–41
42. Lundgren TS. 1972. Slow flow through stationary random beds and suspensions of spheres. *J. Fluid Mech.* 51:273–99
43. Tam CKW. 1969. Drag on a cloud of spherical particles in low reynolds number flow. *J. Fluid Mech.* 38:537–46
44. Guyton AC, Scheel K, Murphree D. 1966. Interstitial fluid pressure. 3. Its effect on resistance to tissue fluid mobility. *Circ. Res.* 19:412–19
45. Rutkowski JM, Moya M, Johannes J, Goldman J, Swartz MA. 2006. Secondary lymphedema in the mouse tail: lymphatic hyperplasia, VEGF-C upregulation, and the protective role of MMP-9. *Microvasc. Res.* 72:161–71
46. Swartz MA, Kaipainen A, Netti PA, Brekken C, Boucher Y, et al. 1999. Mechanics of interstitial-lymphatic fluid transport: theoretical foundation and experimental validation. *J. Biomech.* 32:1297–307
47. Bert JL, Reed RK. 1995. Flow conductivity of rat dermis is determined by hydration. *Biorheology* 32:17–27
48. Mansour JM, Mow VC. 1976. Permeability of articular-cartilage under compressive strain and at high-pressures. *J. Bone Joint Surg. Am.* 58:509–16
49. Bert JL, Reed RK. 1998. Hyaluronan and the flow conductivity of the rat dermis. In *Connective Tissue Biology-Integration and Reductionism*, ed. RK Reed, K Rubin, pp. 41–48. London: Portland Press Ltd
50. McGuire S, Zaharoff D, Yuan F. 2006. Nonlinear dependence of hydraulic conductivity on tissue deformation during intratumoral infusion. *Ann. Biomed. Eng.* 34:1173–81
51. Zhang XY, Luck J, Dewhirst MW, Yuan F. 2000. Interstitial hydraulic conductivity in a fibrosarcoma. *Am. J. Physiol. Heart Circ. Physiol.* 279:H2726–34

52. Happel J. 1959. Viscous flow relative to arrays of cylinders. *AIChE J.* 5:174–77
53. Pedersen JA, Boschetti F, Swartz MA. 2007. Effects of extracellular fiber architecture on cell membrane shear stress in a 3D fibrous matrix. *J. Biomech.* 40:1484–92
54. Scheidegger AE. 1974. *The Physics of Flow Through Porous Media*. Toronto: Univ. Toronto Press
55. Netti PA, Berk DA, Swartz MA, Grodzinsky AJ, Jain RK. 2000. Role of extracellular matrix assembly in interstitial transport in solid tumors. *Cancer Res.* 60:2497–503
56. Overby D, Ruberti J, Gong HY, Freddo TF, Johnson M. 2001. Specific hydraulic conductivity of corneal stroma as seen by quick-freeze/deep-etch. *J. Biomech. Eng.* 123:154–61
57. Diamond SL. 1999. Engineering design of optimal strategies for blood clot dissolution. *Annu. Rev. Biomed. Eng.* 1:427–61
58. Anand S, Wu JH, Diamond SL. 1995. Enzyme-mediated proteolysis of fibrous biopolymers: dissolution front movement in fibrin or collagen under conditions of diffusive or convective transport. *Biotech. Bioeng.* 48:89–107
59. Zakaria ER, Lofthouse J, Flessner MF. 1997. In vivo hydraulic conductivity of muscle: effects of hydrostatic pressure. *Am. J. Physiol. Heart Circ. Physiol.* 42:H2774–82
60. Awwad HK, Elnaggar M, Mocktar N, Barsoum M. 1986. Intercapillary distance measurement as an indicator of hypoxia in carcinoma of the cervix uteri. *Int. J. Rad. Biol.* 12:1329–33
61. Less JR, Skalak TC, Sevick EM, Jain RK. 1991. Microvascular architecture in a mammary-carcinoma—branching patterns and vessel dimensions. *Cancer Res.* 51:265–73
62. Berk DA, Yuan F, Leunig M, Jain RK. 1993. Fluorescence photobleaching with spatial fourier analysis: measurement of diffusion in light-scattering media. *Biophys. J.* 65:2428–36
63. Young ME, Carroad PA, Bell RL. 1980. Estimation of diffusion-coefficients of proteins. *Biotech. Bioeng.* 22:947–55
64. Pluen A, Netti PA, Jain RK, Berk DA. 1999. Diffusion of macromolecules in agarose gels: comparison of linear and globular configurations. *Biophys. J.* 77:542–52
65. Ramanujan S, Pluen A, McKee TD, Brown EB, Boucher Y, Jain RK. 2002. Diffusion and convection in collagen gels: implications for transport in the tumor interstitium. *Biophys. J.* 83:1650–60
66. Wiig H, Kolmannskog O, Tenstad O, Bert JL. 2003. Effect of charge on interstitial distribution of albumin in rat dermis in vitro. *J. Physiol. London* 550:505–14
67. Ogston AG, Preston BN, Wells JD, Ogston AG, Preston BN, et al. 1973. Transport of compact particles through solutions of chain-polymers. *Proc. R. Soc. London Ser. A Mat.* 333:297–316
68. Kosto KB, Deen WM. 2004. Diffusivities of macromolecules in composite hydrogels. *AIChE J.* 50:2648–58
69. Clague DS, Phillips RJ. 1996. Hindered diffusion of spherical macromolecules through dilute fibrous media. *Phys. Fluids* 8:1720–31

70. Phillips RJ. 2000. A hydrodynamic model for hindered diffusion of proteins and micelles in hydrogels. *Biophys. J.* 79:3350–53
71. Brown EB, Boucher Y, Nasser S, Jain RK. 2004. Measurement of macromolecular diffusion coefficients in human tumors. *Microvasc. Res.* 67:231–36
72. Sahimi M. 1992. Transport of macromolecules in porous-media. *J. Chem. Phys.* 96:4718–28
73. Leddy HA, Guilak F. 2003. Site-specific molecular diffusion in articular cartilage measured using fluorescence recovery after photobleaching. *Ann. Biomed. Eng.* 31:753–60
74. Leddy HA. 2004. Molecular diffusion in tissue-engineered cartilage constructs: effects of scaffold material, time, and culture conditions. *J. Biomed. Mat. Res. B* 70B:397–406
75. Evans RC, Quinn TM. 2005. Solute diffusivity correlates with mechanical properties and matrix density of compressed articular cartilage. *Arch. Biochem. Biophys.* 442:1–10
76. Zigmond SH. 1977. Ability of polymorphonuclear leukocytes to orient in gradients of chemotactic factors. *J. Cell Biol.* 75:606–16
77. Fleury ME, Boardman KC, Swartz MA. 2006. Autologous morphogen gradients by subtle interstitial flow and matrix interactions. *Biophys. J.* 91:113–21
78. Deen WM. 1998. *Analysis of Transport Phenomena*. New York: Oxford Univ. Press. 597 pp.
79. Carslaw H, Jaeger J. 1992. *Conduction of Heat in Solids*. Oxford: Oxford Univ. Press
80. Johnston ST, Deen WM. 1999. Hindered convection of proteins in agarose gels. *J. Membr. Sci.* 153:271–79
81. Kosto KB, Deen WM. 2005. Hindered convection of macromolecules in hydrogels. *Biophys. J.* 88:277–86
82. Brissova M, Petro M, Lacik I, Powers AC, Wang T. 1996. Evaluation of microcapsule permeability via inverse size exclusion chromatography. *Anal. Biochem.* 242:104–11
83. Reddy ST, Berk DA, Jain RK, Swartz MA. 2006. A sensitive in vivo model for quantifying interstitial convective transport of injected macromolecules and nanoparticles. *J. App. Physiol.* 101:1162–69
84. Evans RC, Quinn TM. 2006. Solute convection in dynamically compressed cartilage. *J. Biomech.* 39:1048–55
85. Reddy ST, Rehor A, Schmoekel HG, Hubbell JA, Swartz MA. 2006. In vivo targeting of dendritic cells in lymph nodes with poly(propylene sulfide) nanoparticles. *J. Cont. Rel.* 112:26–34
86. Yuan F, Krol A, Tong S. 2001. Available space and extracellular transport of macromolecules: effects of pore size and connectedness. *Ann. Biomed. Eng.* 29:1150–58
87. Park JE, Keller GA, Ferrara N. 1993. Vascular endothelial growth-factor (VEGF) isoforms—differential deposition into the subepithelial extracellular-matrix and bioactivity of extracellular matrix-bound VEGF. *Mol. Biol. Cell* 4:1317–26

88. Uchimura K, Morimoto-Tomita M, Bistrup A, Li J, Lyon M, et al. 2006. HSulf-2, an extracellular endosulfatase, is secreted by MCF-7 breast carcinoma cells and selectively mobilizes heparin-bound VEGF, FGF-1, and SDF-1. *FASEB J.* 20:A1364
89. Gengrinovitch S, Berman B, David G, Witte L, Neufeld G, Ron D. 1999. Glypican-1 is a VEGF(165) binding proteoglycan that acts as an extracellular chaperone for VEGF(165). *J. Biol. Chem.* 274:10816–22
90. Dowd CJ, Cooney CL, Nugent MA. 1999. Heparan sulfate mediates BFGF transport through basement membrane by diffusion with rapid reversible binding. *J. Biol. Chem.* 274:5236–44
91. Nugent MA, Edelman ER. 1992. Kinetics of basic fibroblast growth-factor binding to its receptor and heparan-sulfate proteoglycan—a mechanism for cooperativity. *Biochemistry* 31:8876–83
92. Sahni A, Odrljin T, Francis CW. 1998. Binding of basic fibroblast growth factor to fibrinogen and fibrin. *J. Biol. Chem.* 273:7554–59
93. Hirose J, Kawashima H, Yoshie O, Tashiro K, Miyasaka M. 2001. Versican interacts with chemokines and modulates cellular responses. *J. Biol. Chem.* 276:5228–34
94. Patel DD, Koopmann W, Imai T, Whichard LP, Yoshie O, Krangel MS. 2001. Chemokines have diverse abilities to form solid phase gradients. *Clin. Immun.* 99:43–52
95. Dhoot GK, Gustafsson MK, Ai XB, Sun WT, Standiford DM, Emerson CP. 2001. Regulation of WNT signaling and embryo patterning by an extracellular sulfatase. *Science* 293:1663–66
96. Houck KA, Leung DW, Rowland AM, Winer J, Ferrara N. 1992. Dual regulation of vascular endothelial growth-factor bioavailability by genetic and proteolytic mechanisms. *J. Biol. Chem.* 267:26031–37
97. Lee S, Jilani SM, Nikolova GV, Carpizo D, Iruela-Arispe ML. 2005. Processing of VEGF-A by matrix metalloproteinases regulates bioavailability and vascular patterning in tumors. *J. Cell Biol.* 169:681–91
98. Sahni A, Guo M, Sahni SK, Francis CW. 2004. Interleukin-1 beta but not IL-1 alpha binds to fibrinogen and fibrin and has enhanced activity in the bound form. *Blood* 104:409–14
99. Sahni A, Sahni SK, Simpson-Haidaris PJ, Francis CW. 2004. Fibrinogen binding potentiates FGF-2 but not VEGF induced expression of u-PA, u-PAR, and PAI-1 in endothelial cells. *J. Thromb. Haem.* 2:1629–36
100. Keuren JFW, Baruch D, Legendre P, Denis CV, Lenting PJ, et al. 2004. Von willebrand factor C1C2 domain is involved in platelet adhesion to polymerized fibrin at high shear rate. *Blood* 103:1741–46
101. Reis RCM, Schuppan D, Barreto AC, Bauer M, Bork JP, et al. 2005. Endostatin competes with BFGF for binding to heparin-like glycosaminoglycans. *Biochem. Biophys. Res. Comm.* 333:976–83
102. Yasui N, Mori T, Morito D, Matsushita O, Kourai H, et al. 2003. Dual-site recognition of different extracellular matrix components by antiangiogenic/neurotrophic serpin, PEDF. *Biochemistry* 42:3160–67

103. Cohen I, Pappo O, Elkin M, San T, Bar-Shavit R, et al. 2006. Heparanase promotes growth, angiogenesis and survival of primary breast tumors. *Int. J. Cancer* 118:1609–17
104. Goldshmidt O, Zcharia E, Abramovitch R, Metzger S, Aingorn H, et al. 2002. Cell surface expression and secretion of heparanase markedly promote tumor angiogenesis and metastasis. *Proc. Natl. Acad. Sci. USA* 99:10031–36
105. Morimoto-Tomita M, Uchimura K, Bistrup A, Lum DH, Egeblad M, et al. 2005. Sulf-2, a proangiogenic heparan sulfate endosulfatase, is upregulated in breast cancer. *Neoplasia* 7:1001–10
106. Elkin M, Ilan N, Ishai-Michaeli R, Friedmann Y, Papo O, et al. 2001. Heparanase as mediator of angiogenesis: mode of action. *FASEB J.* 15(9):1661–63
107. Hall H, Baechi T, Hubbell JA. 2001. Molecular properties of fibrin-based matrices for promotion of angiogenesis in vitro. *Microvasc. Res.* 62:315–26
108. Zisch AH, Schenk U, Schense JC, Sakiyama-Elbert SE, Hubbell JA. 2001. Covalently conjugated VEGF-fibrin matrices for endothelialization. *J. Cont. Rel.* 72:101–13
109. DeWitt A, Iida T, Lam HY, Lauffenburger DA. 2002. Affinity regulates spatial range of EGF receptor autocrine ligand binding. *Dev. Biol.* 250:305–16
110. Shvartsman SY, Wiley HS, Deen WM, Lauffenburger DA. 2001. Spatial range of autocrine signaling: modeling and computational analysis. *Biophys. J.* 81:1854–67
111. Tschumperlin DJ, Dai GH, Maly IV, Kikuchi T, Laiho LH, et al. 2004. Mechanotransduction through growth-factor shedding into the extracellular space. *Nature* 429:83–86
112. Van Meerveld J, Molenaar MM, Huyghe JM, Baaijens FPT. 2003. Analytical solution of compression, free swelling and electrical loading of saturated charged porous media. *Tranport. Porous Med.* 50:111–26
113. Hellmich C, Ulm FJ. 2005. Drained and undrained poroelastic properties of healthy and pathological bone: a poro-micromechanical investigation. *Transport. Porous Med.* 58:243–68
114. Sengers BG, Oomens CWJ, Baaijens FPT. 2004. An integrated finite-element approach to mechanics, transport and biosynthesis in tissue engineering. *J. Biomech. Eng. Trans. ASME* 126:82–91
115. Guyton AC, Prather J, Scheel K, McGehee J. 1966. Interstitial fluid pressure. 4. Its effect on fluid movement through capillary wall. *Circ. Res.* 19:1022
116. Levick JR. 1991. A 2-dimensional morphometry-based model of interstitial and transcapillary flow in rabbit synovium. *Exp. Physiol.* 76:905–21
117. Dreher MR, Liu WG, Michelich CR, Dewhirst MW, Yuan F, Chilkoti A. 2006. Tumor vascular permeability, accumulation, and penetration of macromolecular drug carriers. *J. Nat. Canc. Inst.* 98:335–44
118. Tabata T, Murakami Y, Ikada Y. 1998. Tumor accumulation of poly(vinyl alcohol) of different sizes after intravenous injection. *J. Cont. Rel.* 50:123–33
119. Baish JW, Netti PA, Jain RK. 1997. Transmural coupling of fluid flow in microcirculatory network and interstitium in tumors. *Microvasc. Res.* 53:128–41

120. Eikenes L, Bruland OS, Brekken C, Davies CDL. 2004. Collagenase increases the transcapillary pressure gradient and improves the uptake and distribution of monoclonal antibodies in human osteosarcoma xenografts. *Cancer Res.* 64:4768–73
121. Wang Y, Yuan F. 2006. Delivery of viral vectors to tumor cells: extracellular transport, systemic distribution, and strategies for improvement. *Ann. Biomed. Eng.* 34:114–27
122. Brekken C, Hjelstuen MH, Bruland OS, Davies CD. 2000. Hyaluronidase-induced periodic modulation of the interstitial fluid pressure increases selective antibody uptake in human osteosarcoma xenografts. *Anticanc. Res.* 20:3513–19
123. Chang C, Werb Z. 2001. The many faces of metalloproteases: cell growth, invasion, angiogenesis and metastasis. *Trends Cell Biol.* 11:S37–43
124. Stamenkovic I. 2000. Matrix metalloproteinases in tumor invasion and metastasis. *Sem. Cancer Biol.* 10:415–33
125. Reddy ST, Swartz MA, Hubbell JA. 2006. Targeting dendritic cells with biomaterials: developing the next generation of vaccines. *Trends Immun.* 27(12):573–79
126. Turing AM. 1952. The chemical basis of morphogenesis. *Philos. Trans. R. Soc. London B* 237:37–72
127. Quinn TM, Grodzinsky AJ, Buschmann MD, Kim YJ, Hunziker EB. 1998. Mechanical compression alters proteoglycan deposition and matrix deformation around individual cells in cartilage explants. *J. Cell Sci.* 111:573–83
128. Ng CP, Hinz B, Swartz MA. 2005. Interstitial fluid flow induces myofibroblast differentiation and collagen alignment in vitro. *J. Cell Sci.* 118:4731–39
129. Tarbell JM, Weinbaum S, Kamm RD. 2005. Cellular fluid mechanics and mechanotransduction. *Ann. Biomed. Eng.* 33:1719–23
130. Ingber DE. 2006. Cellular mechanotransduction: putting all the pieces together again. *FASEB J.* 20:811–27
131. Maly IV, Lee RT, Lauffenburger DA. 2004. A model for mechanotransduction in cardiac muscle: effects of extracellular matrix deformation on autocrine signaling. *Ann. Biomed. Eng.* 32:1319–35
132. Shields JD, Fleury ME, Yong C, Tomei AA, Randolph GJ, Swartz MA. 2007. Autologous chemotaxis as a mechanism of tumor cell homing to lymphatics via interstitial flow and autocrine CCL21. *Cancer Cell.* In press
133. Shiratori H, Hamada H, 2006. The left-right axis in the mouse: from origin to morphology. *Dev.* 133(11):2095–104
134. Sadler JE. 1998. Biochemistry and genetics of von Willebrand factor. *Annu. Rev. Biochem.* 67:395–424
135. Trudnowski RJ, Rico RC. 1974. Specific gravity of blood and plasma at 4 and 37°C. *Clin. Chem.* 20:615–16

Annual Review
of Biomedical
Engineering

Volume 9, 2007

Contents

Indexes

Errata

An online log of corrections to *Annual Review of Biomedical Engineering* chapters (if any, 1977 to the present) may be found at http://bioeng.annualreviews.org/